Contribution from the Department of Chemistry,
The University of North Carolina, Chapel Hill, North Carolina 27599-3290

Formation of a Metal-Hydride Bond and the Insertion of CO_2. Key Steps in the Electrocatalytic Reduction of Carbon Dioxide to Formate Anion

J. Richard Pugh, Mitchell R. M. Bruce, B. Patrick Sullivan,* and Thomas J. Meyer*

Received April 24, 1990

The complex *cis*-$[Ru(bpy)_2(CO)H]^+$ was shown to be a catalyst for the electrochemical reduction of CO_2 in CH_3CN with added water. One product of the reduction is the formate anion. It is formed in a catalytic cycle which involves (1) one-electron, bpy-based reduction of *cis*-$[Ru(bpy)_2(CO)H]^+$ (2) insertion of CO_2 into the Ru-H bond to give the once-reduced formato complex *cis*-$[Ru(bpy)_2(CO)(OC(O)H)]^0$, and (3) a subsequent, one-electron reduction of this complex, which leads to the loss of formate anion and the re-formation of *cis*-$[Ru(bpy)_2(CO)H]^+$ by the reduction of H_2O. The formation of the hydrido complex following the two-electron reduction of either the formato complex or the acetonitrilo complex *cis*-$[Ru(bpy)_2(CO)(NCCH_3)]^{2+}$ was demonstrated independently. A second major pathway for the reduction of CO_2 was identified, which gave CO as a product. The mechanism of this reaction, which was identified earlier for *cis*-$[Os(bpy)_2(CO)H]^+$, appears to involve associative attack of CO_2 on the twice-reduced formato or acetonitrilo complexes.

Introduction

Polypyridyl ligands such as 2,2'-bipyridine or 1,10-phenanthroline have found application in homogeneous catalysis either as reducible, electron "reservoirs" in metal complexes[1] or as promoters of catalytic reactions.[2] One reaction in which they have been shown to play a role is in the reduction of CO_2.[3] Certain polypyridyl complexes of the second- and third-row transition metals have been reported to act as catalysts for the electrochemical reduction of CO_2. In some cases, the results of mechanistic studies have given insight into how these reactions occur and into those factors that determine the selectivities and efficiencies of product formation.[1c-g]

Polypyridyl complexes of ruthenium[4] have been implicated as active catalysts in the water-gas shift reaction[5] and in the reduction of CO_2 to formate.[6] It has been suggested by Lehn and co-workers that $[Ru(bpy)_2(CO)H]^+$ is the active catalyst in the photochemical reduction of CO_2 to formate by triethanolamine in DMF, a reaction that utilizes $[Ru(bpy)_3]^{2+}$ as the photosensitizer.[7]

We report here the results of cyclic voltammetric and controlled-potential electrolysis studies on $[Ru(bpy)_2(CO)H]^+$ in CO_2-saturated CH_3CN with added water. Under these conditions the complex acts as a catalyst for the electrochemical reduction of CO_2 to formate anion and CO. Two key mechanistic steps have been identified in the reduction of CO_2 to formate. The first is the insertion of CO_2 into the metal-hydride bond to give the corresponding formato complex. This reaction is initiated by a one-electron reduction at bpy. The second step is the re-formation of the metal-hydride bond by the reduction of water. This reaction occurs following the insertion of CO_2 and a second, one-electron reduction. Each step plays a key role in the electrocatalyzed reduction of CO_2 to formate.

Experimental Section

Materials. Acetonitrile (Burdick and Jackson) for the electrochemical experiments was used as received. Deuteriated acetonitrile was purchased from Cambridge Isotope Laboratories. All other solvents were reagent grade and were purchased from Aldrich Chemical Co. Tetra-*n*-butylammonium hexafluorophosphate (TBAH) was prepared by the metathesis of tetra-*n*-butylammonium bromide and HPF_6 in water and was purified by successive recrystallizations from ethanol/water and dichloromethane/diethyl ether followed by drying in vacuo at 80 °C. Potassium hexafluorophosphate was dried in vacuo at 80 °C. The CO_2 was Air Products research grade (99.995%). The $^{13}CO_2$ was generated by the slow addition of trifluoroacetic anhydride (Aldrich) to $Ba^{13}CO_3$ (Aldrich). The ruthenium complexes were prepared by literature methods.[4]

Electrochemical Measurements. Cyclic voltammetric (CV) experiments were conducted by using a Princeton Applied Research (PAR) Model 173 potentiostat, in conjunction with either a homebuilt sweep generator or a PAR Model 175 universal programmer, and a Hewlett-Packard Model 7015B X-Y recorder. All electrochemical measurements were made within a Vacuum Atmospheres drybox. Approximately 5 mL of 0.1 M TBAH/CH_3CN or a 0.2 M TBAH/1,2-difluorobenzene solution was added to a three-compartment cell that had ground-glass frits separating the working, auxiliary, and reference compartments. The electrodes were a 0.12 cm diameter Pt disk as the working electrode, a Pt-wire auxiliary electrode, and a saturated sodium chloride calomel reference electrode (SSCE). The $E_{1/2}$ values were calculated from the average of the cathodic and anodic peak potentials. Prior to each measurement, the solution was purged with either N_2 or CO_2 that had been presaturated with CH_3CN. Microelectrode cyclic voltammetry[8] was conducted with the use of a PAR 175 universal programmer as a sweep generator, a Tektronix 2230 digital oscilloscope, and a two-electrode cell arrangement that was similar to previously described systems.[8c,d] The microelectrodes were prepared by standard literature techniques.[8a]

Controlled-potential electrolysis experiments were performed in a three-compartment cell that was designed for handling air-sensitive materials as well as for sampling the gases above the electrolysis solution.[1c] The working electrode was constructed of either platinum mesh

(1) (a) Sullivan, B. P.; Conrad, D.; Meyer, T. J. *Inorg. Chem.* **1985**, *24*, 3640. (b) Abruna, H. D.; Teng, A. Y.; Samuels, G. J.; Meyer, T. J. *J. Am. Chem. Soc.* **1979**, *101*, 6745. (c) Sullivan, B. P.; Bolinger, C. M.; Conrad, D.; Vining, W. J.; Meyer, T. J. *J. Chem. Soc., Chem. Commun.* **1985**, 1414. (d) Bolinger, C. M.; Sullivan, B. P.; Conrad, D.; Gilbert, J. A.; Story, N.; Meyer, T. J. *J. Chem. Soc., Chem. Commun.* **1985**, 796. (e) Bolinger, C. M.; Story, N.; Sullivan, B. P.; Meyer, T. J. *Inorg. Chem.* **1988**, *27*, 4582. (f) Bruce, M. R. M.; Megehee, E.; Sullivan, B. P.; Thorp, H.; O'Toole, T. R.; Downard, A.; Meyer, T. J. *Organometallics* **1988**, *7*, 238. (g) Bruce, M. R. M.; Megehee, E.; Sullivan, B. P.; Thorp, H.; O'Toole, T. R.; Pugh, J. R.; Meyer, T. J. Manuscript in preparation.

(2) Alessio, E.; Zassinovich, G.; Mestroni, G. *J. Mol. Catal.* **1983**, *18*, 113. See also: Alessio, E.; Clauti, G.; Mestroni, G. *J. Mol. Catal.* **1985**, *29*, 77.

(3) (a) Sullivan, B. P.; Bruce, M. R. M.; O'Toole, T. R.; Bolinger, C. M.; Megehee, E.; Thorp, H.; Meyer, T. J. *Adv. Chem. Ser.* **1988**, *363*, 52. (b) O'Connell, G.; Hommeltoft, S. I.; Eisenberg, R. In *Carbon Dioxide as a Source of Carbon*; Aresta, M., Forti, G., Eds.; Reidel Publishing Co.: Dordrecht, The Netherlands, 1987. (c) Sullivan, B. P.; Meyer, T. J. *Organometallics* **1986**, *5*, 1500.

(4) (a) Kelly, J. M.; Vos, J. G. *Angew. Chem., Int. Ed. Engl.* **1982**, *21*, 628. (b) Caspar, J. V.; Sullivan, B. P.; Meyer, T. J. *Organometallics* **1983**, *2*, 55. (c) Sullivan, B. P.; Caspar, J. V.; Johnson, S. R.; Meyer, T. J. *Organometallics* **1984**, *3*, 1241. (d) Kelly, J. M.; Vos, J. G. *J. Chem. Soc., Dalton Trans.* **1986**, 1045. (e) Megehee, E. Ph.D. Dissertation, University of North Carolina, Chapel Hill, 1986.

(5) (a) Choudhurry, D.; Cole-Hamilton, D. *J. Chem. Soc., Dalton Trans.* **1982**, 1885. (b) Haasnoot, J. G.; Hinrichs, W.; Weir, O.; Vos, J. G. *Inorg. Chem.* **1986**, *25*, 1440. (c) Tanaka, K.; Morimoto, M.; Tanaka, T. *Chem. Lett.* **1983**, 901.

(6) (a) Ishida, H.; Tanaka, K.; Tanaka, T. *Chem. Lett.* **1985**, 405. (b) Ishida, H.; Tanaka, K.; Morimoto, M.; Tanaka, T. *Organometallics* **1986**, *5*, 724. (c) Ishida, H.; Tanaka, K.; Tanaka, T. *Organometallics* **1987**, *6*, 181.

(7) Hawecker, J.; Lehn, J.-M.; Ziessel, R. *J. Chem. Soc., Chem. Commun.* **1985**, 56.

(8) (a) Howell, J. O.; Wightman, R. M. *Anal. Chem.* **1984**, *56*, 524. (b) Wipf, D. O.; Kristensen, E. W.; Deakin, M. R.; Wightman, R. M. *Anal. Chem.* **1988**, *60*, 306. (c) Montenegro, M. I.; Pletcher, D. *J. Electroanal. Chem. Interfacial Electrochem.* **1986**, *200*, 371. (d) Howell, J. O.; Goncalves, J. M.; Amatore, C.; Klasinc, L.; Wightman, R. M.; Kochi, J. K. *J. Am. Chem. Soc.* **1984**, *106*, 3968. (e) Wightman, R. M. *Anal. Chem.* **1981**, *53*, 1125A.

0020-1669/91/1330-0086$02.50/0

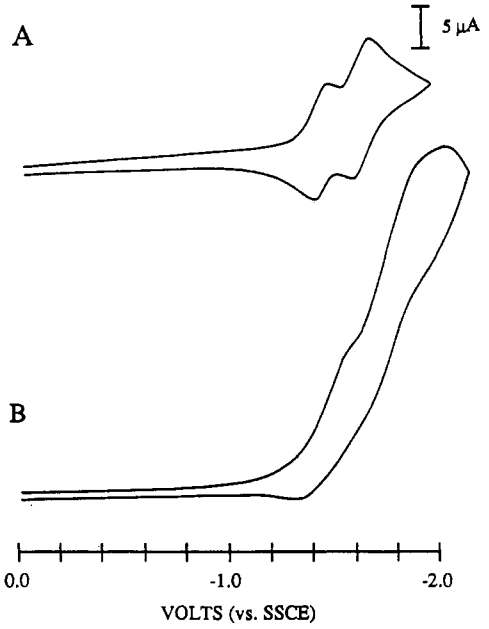

Figure 1. Cyclic voltammograms of a solution 1.0×10^{-3} M in *cis*-$[Ru(bpy)_2(CO)H](PF_6)$ in 0.1 M TBAH/CH_3CN with a Pt-disk working electrode at a scan rate of 100 mV/s: (A) reductive scan under an atmosphere of N_2; (B) reductive scan under an atmosphere of CO_2.

or vitreous carbon. The reference electrode was a SSCE attached to the main compartment via a Luggin probe. The auxiliary electrode was a Pt-mesh electrode that was separated from the main compartment by a fine ground-glass frit. The main and auxiliary compartments were connected in such a way as to allow the gasses, but not the solutions, to mix. For this cell configuration the total gas volume of the main and auxiliary compartments was 70 mL when 35 mL of solution was present.

In a typical electrolysis experiment, the apparatus was oven-dried and assembled inside a drybox. The electrolyte solution was introduced and saturated with the appropriate gas by bubble-degassing for a minimum of 15 min.[9] At this point the background current was measured. The catalyst was introduced, and the solution was purged with the appropriate gas for 15–30 min. The controlled-potential electrolyses, which generally took from 40–70 min, were conducted at the potentials indicated in the Results section.

Analyses. After completion of an electrolysis run, several different analyses were conducted. Gas samples were analyzed by using a Hewlett-Packard model 5890A gas chromatograph equipped with a thermal conductivity detector. Analysis for CO employed a 5-Å molecular sieve column with He as the carrier gas. Analysis for H_2 was carried out with a 5-Å molecular sieve column with Ar as the carrier gas. Analyses for CO_2 and H_2O were carried out on a Porapak Q column with He as the carrier gas.[9] Acetonitrile solutions saturated with CO_2 were typically found to be 0.14 M in CO_2. Spectroscopic grade CH_3CN from Burdick and Jackson contained trace water that in some cases was used as the proton source for the electrocatalytic runs and cyclic voltammetric experiments. In this case, the water concentration was usually found to be ~1 mM. Unless otherwise noted, the concentration of H_2O was ~5 mM in the experiments described here.

UV–visible spectral measurements were made with a Hewlett-Packard Model 8451A diode array spectrophotometer by employing a 1 cm path length quartz cuvette. Fourier-transform infrared (FTIR) measurements were made with a Nicolet model 20DX FTIR spectrophotometer and a 0.1 mm path length NaCl solution cell. Calibration curves were utilized where the integrated areas under ν(CO) bands were used to determine product concentrations.

Analyses for anionic products utilized a Dionex Model 2000i ion chromatograph. Prior to this analysis, the samples were treated in the following manner: (1) Enough distilled water was added to dilute the sample to a 2:1 (v:v) H_2O to CH_3CN ratio. (2) The CH_3CN/H_2O azeotrope was removed by using a rotary evaporator at room temperature. (3) The analysis was conducted on the aqueous solution that remained following filtration through Q5 (Fisher) grade filter paper. Control experiments with standard solutions containing Cl^-, Br^-, oxalate, glycolate, glyoxalate, or formate showed an average recovery of 92 ± 8% by using this procedure.

(9) Hogen, J.; Engel, R.; Stevenson, H. *Anal. Chem.* **1970**, *42*, 249.

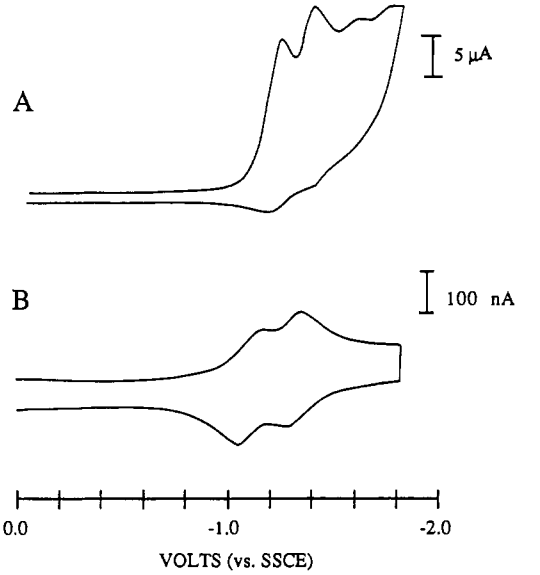

Figure 2. Cyclic voltammograms of solution containing *cis*-$[Ru(bpy)_2(CO)(NCCH_3)](PF_6)_2$ in 0.1 M TBAH/CH_3CN, which was 5 mM in added H_2O, at a Pt-disk working electrode: (A) reductive scan for a solution 2.0×10^{-3} M in complex at 100 mV/s; (B) reductive scan for a solution that was 1.0×10^{-3} M in complex at a scan rate of 1000 V/s.

Results

Cyclic Voltammetry. A cyclic voltammogram of a solution containing *cis*-$[Ru(bpy)_2(CO)H](PF_6)$ in 0.1 M TBAH/CH_3CN at a scan rate of 100 mV/s is shown in Figure 1A. Reversible redox processes appear at $E_{1/2} = -1.45$ and -1.65 V vs SSCE, arising from sequential reduction of the two bipyridyl ligands.[4c] Upon saturation of the solution with CO_2, a dramatic increase in peak current occurs at both waves (Figure 1B). A cyclic voltammogram of *cis*-$[Ru(bpy)_2(CO)H]^+$ in 0.1 M TBAH/CH_3CN solution with added formate anion showed no current enhancement at either wave.

In Figure 2 are shown cyclic voltammograms of a solution containing *cis*-$[Ru(bpy)_2(CO)(NCCH_3)](PF_6)_2$ in 0.1 M TBAH/CH_3CN in the presence of 5 mM H_2O. At 100 mV/s (Figure 2A), four reduction waves are observed. They appear at $E_{p,c} = -1.20$ ($E_{1/2} = -1.15$), -1.40($E_{1/2} = -1.35$), -1.55, and -1.75 V. The first two reductions are the bpy-based reductions of the starting complex. The second two are the bpy-based reductions of the hydrido complex that forms upon two-electron reduction of the acetonitrile complex. If the reductive span is reversed after the first reduction at -1.25 V, a reversible wave is observed, signaling the absence of a reaction leading to the hydrido complex. If the scan rate is increased to 1000 V/s (Figure 2B), the formation of *cis*-$[Ru(bpy)_2(CO)H]^+$ is suppressed and only the waves for the *cis*-$[Ru(bpy)_2(CO)(NCCH_3)]^{2+}$-based couples are observed.

Cyclic voltammograms of a solution containing *cis*-$[Ru(bpy)_2(CO)(OC(O)H)](PF_6)$ in 0.1 M TBAH/CH_3CN in the presence of 5 mM H_2O are shown in Figure 3 under a variety of scan conditions. The same pattern of waves was observed as for *cis*-$[Ru(bpy)_2(CO)(NCCH_3)]^{2+}$. The pattern was less well defined because the second reduction of the formato complex at $E_{1/2} = -1.50$ V overlaps with the first reduction of the hydrido complex. At a scan rate of 100 mV/s, the first bpy-based reduction at $E_{1/2} = -1.30$ V is reversible (Figure 3B). If the scan is continued past the second reduction, *cis*-$[Ru(bpy)_2(CO)H]^+$ appears as a product (Figure 3A). At a scan rate of 1000 V/s, both reductions for $[Ru(bpy)_2(CO)(OC(O)H)]^+$ are chemically reversible.

Cyclic voltammograms of solutions containing $[Ru(bpy)_2(CO)(OC(O)H)](PF_6)$ in the inert, noncoordinating solvent 1,2-difluorobenzene,[10] 0.2 M in TBAH, showed the same pattern of

(10) O'Toole, T. R.; Younathan, J. N.; Sullivan, B. P.; Meyer, T. J. *Inorg. Chem.* **1989**, *28*, 3923.

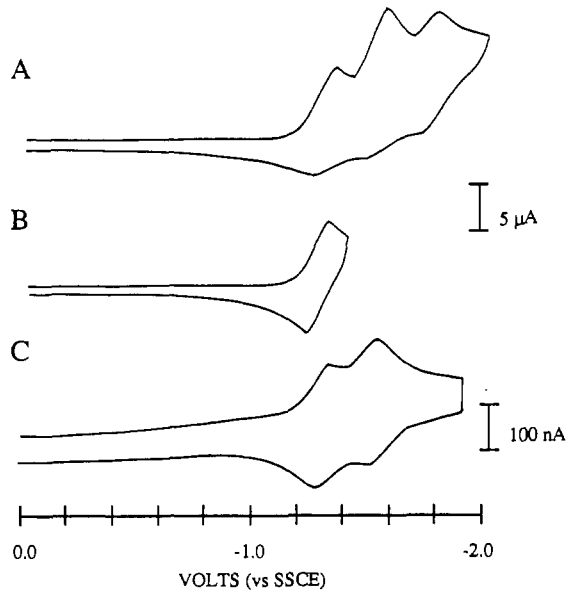

Figure 3. Cyclic voltammograms of a solution 1.0×10^{-3} M in *cis*-$[Ru(bpy)_2(CO)(OC(O)H)](PF_6)$ in 0.1 M TBAH/CH_3CN with 5 mM added H_2O: (A) reductive scan at 100 mV/s scan rate; (B) reductive scan at 100 mV/s that was switched past the first bpy-based reduction; (C) reductive scan at 1000 V/s. The working electrode was a Pt disk.

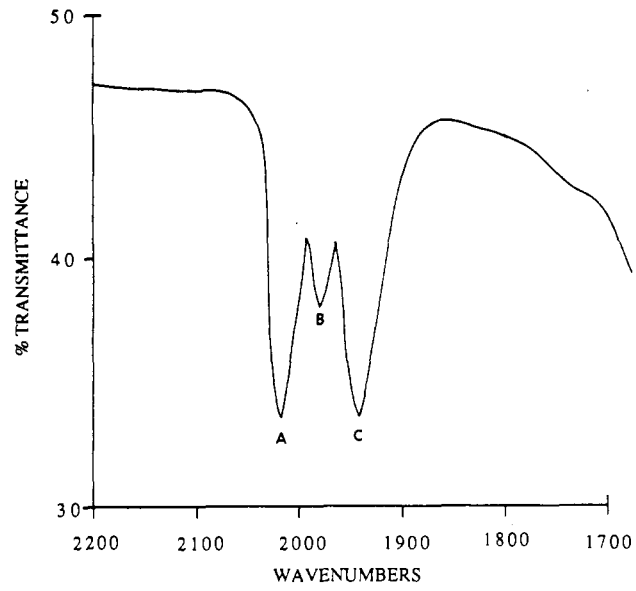

Figure 4. Fourier transform infrared spectrum in the ν(CO) region of an electrolysis solution which contained initially 1.2×10^{-3} M $[Ru(bpy)_2(CO)H](PF_6)$ and 0.32 M added water in 0.1 M TBAH/CH_3CN. The features labeled in the spectrum arise from the ν(CO) bands in (A) *cis*-$[Ru(bpy)_2(CO)(NCCH_3)]^{2+}$, (B) *cis*-$[Ru(bpy)_2(CO)(OC(O)H)]^+$, and (C) *cis*-$[Ru(bpy)_2(CO)H]^+$.

reduction waves ($E_{p,c}$ = −1.35, −1.52, −1.75 V vs SSCE) as in TBAH/acetonitrile. From this observation it can be inferred that the hydrido complex can form by direct attack of residual water (~10 mM in the case of 1,2-difluorobenzene by GC) in the solvent on the twice-reduced formato complex $[Ru(bpy)_2(CO)(OC(O)H)]^-$ without the intervention on an intermediate solvento complex. As noted by a reviewer, on the basis of this result alone, we cannot rule out reductively induced loss of CO_2 to give back the hydrido complex. However, the rapid formation of the hydrido complex from $[Ru(bpy)_2(CO(NCCH_3)]^0$ shows that the reduced complexes can react with water to re-form the hydride, even in the absence of formate.

Controlled-Potential Electrolyses: *cis*-$[Ru(bpy)_2(CO)H]^+$ in the Presence of CO_2. Controlled-potential electrolyses were conducted on CO_2-saturated solutions of 0.1 M TBAH/CH_3CN to which the complex and varying amounts of water had been added. In these studies the concentration range in *cis*-$[Ru(bpy)_2(CO)H](PF_6)$ was 3.0×10^{-4} to 1.2×10^{-3} M. The water concentration was varied from 3.0 mM to 0.40 M. The number of 2 electron equiv turnovers per catalyst molecule ranged from 4.8 to 28.2. The electrolysis potentials were varied from −1.3 to −1.6 V vs SSCE.

Analysis of the ionic products from seven runs gave an average value of 17% for the current efficiency in formate anion with no systematic trends with electrolysis time or amount of added water. Other detected products were CO (57% on average) and H_2 (8% on average). The remainder of the current efficiencies (18%) were not accounted for. Other possible CO_2 reduction products, such as oxalate, methanol, methane, and formaldehyde, were not detected in solution. The formation of H_2 as a product appears to occur by the direct reduction of water at the platinum working electrode. Electrolysis of 0.1 M TBAH/CH_2CN solutions with no added water led to the production of H_2 by reduction of the residual water (~1 mM) in the solution. Electrolyses of $[Ru(bpy)_2(CO)H]^+$ in CO_2-saturated 0.1 M TBAH/CH_3CN solutions at a carbon electrode gave only CO and formate as products; no H_2 evolution was detected.

The FTIR spectrum of a CO_2-saturated solution after electrolysis (1.2×10^{-3} M catalyst, 0.30 M H_2O, −1.3 V, 13 turnovers) showed the presence of ν(CO) bands for *cis*-$[Ru(bpy)_2(CO)(NCCH_3)]^{2+}$ (2015 cm^{-1}), *cis*-$[Ru(bpy)_2(CO)(OC(O)H)]^+$ (1984 cm^{-1}), and *cis*-$[Ru(bpy)_2(CO)H]^+$ (1938 cm^{-1}) (Figure 4). The UV–visible spectrum of the electrolysis solution was complex but consistent with the presence of the acetonitrilo, formato, and hydrido complexes with λ_{max} = 370 nm (ϵ = 5750 M^{-1} cm^{-1}), 408 nm (4550 M^{-1} cm^{-1}), and 452 nm (3370 M^{-1} cm^{-1}), respectively. An additional product appeared in the solution with λ_{max} = 584 nm. It was identified as $[Ru(bpy)_2(CO_3)]$ by comparison with an authentic sample, and by the observation that addition of HPF_6 to either the electrolysis solution or to a solution containing $[Ru(bpy)_2(CO_3)]$ led to $[Ru(bpy)_2(NCCH_3)_2]^{2+}$, λ_{max} = 426 nm (ϵ = 8600 M^{-1} cm^{-1}).[11]

***cis*-$[Ru(bpy)_2(CO)H]^+$ in the Presence of $^{13}CO_2$.** A solution of $[Ru(bpy)_2(CO)H]^+$ in $^{13}CO_2$-saturated 0.1 M TBAH/CH_3CN was reduced at −1.3 V for 11.5 turnovers of the catalyst. The FTIR spectrum of the electrolysis solution showed the presence of $[Ru(bpy)_2(CO)(NCCH_3)]^{2+}$, $[Ru(bpy)_2(CO)(OC(O)H)]^+$, and $[Ru(bpy)_2(CO)H]^+$ at ν(CO) = 2015, 1984, and 1938 cm^{-1}. No additional FTIR peaks were present in the carbonyl region.

Formation of *cis*-$[Ru(bpy)_2(CO)H]^+$ by Electrochemical Reduction. (1) Of *cis*-$[Ru(bpy)_2(CO)(OC(O)H)]^+$. Upon controlled-potential electrolysis of *cis*-$[Ru(bpy)_2(CO)(OC(O)H)](PF_6)$ at −1.40 V in 0.1 M TBAH/CH_3CN, which was ~5 mM in H_2O, *cis*-$[Ru(bpy)_2(CO)H]^+$ appeared as the major product. Under an atmosphere of dinitrogen, 2 electron equiv were required for the electrolysis to reach completion. Under CO_2, the reduction of *cis*-$[Ru(bpy)_2(CO)(OC(O)H)]^+$ became catalytic, and the formato and acetonitrilo complexes also appeared in the solution as minor products.

(2) Of *cis*-$[Ru(bpy)_2(CO)(NCCH_3)]^{2+}$. Controlled-potential electrolyses of $[Ru(bpy)_2(CO)(NCCH_3)](PF_6)_2$ at −1.3 or -1.6 V vs SSCE in either N_2- or CO_2-saturated 0.1 M TBAH/CH_3CN led to *cis*-$[Ru(bpy)_2(CO)H]^+$. Under CO_2, the reduction was catalytic and $[Ru(bpy)_2(CO_3)]$ appeared in the solution after electrolysis. Under dinitrogen, the reduction of $[Ru(bpy)_2(CO)(NCCH_3)]^{2+}$ occurred with the consumption of 2 electron equiv and led to *cis*-$[Ru(bpy)_2(CO)H]^+$ quantitatively.

***cis*-$Ru(bpy)_2(CO)(CH_2Ph)]^+$ in the Presence of CO_2.** Controlled-potential electrolyses of *cis*-$[Ru(bpy)_2(CO)(CH_2Ph)](PF_6)$ in the presence of CO_2 were performed under conditions similar to those described for *cis*-$[Ru(bpy)_2(CO)H](PF_6)$. In a typical experiment (3.7×10^{-4} M catalyst, 0.25 M H_2O, −1.5 V, 20.7

(11) (a) Brown, G. M.; Callahan, R. W.; Meyer, T. J. *Inorg. Chem.* **1975**, *14*, 1915. (b) Johnson, E. C.; Sullivan, B. P.; Salmon, D. J.; Adeyemi, S. A.; Meyer, T. J. *Inorg. Chem.* **1978**, *17*, 2211.
(12) Moore, E. J.; Sullivan, J. M.; Norton, J. R. *J. Am. Chem. Soc.* **1986**, *108*, 2257.

turnovers, C electrode), the current efficiencies for the formation of CO and formate anion were 74% and 2.5%, respectively. The remaining electron equivalents were not accounted for. At the end of the electrolysis period, an FTIR spectrum of the solution showed that *cis*-$[Ru(bpy)_2(CO)(CH_2Ph)]^+$ (ν(CO) = 1935 cm^{-1}) was the only carbonyl-containing complex in the solution.

***cis*-$[Ru(bpy)_2(NCCH_3)_2]^{2+}$ in the Presence of CO_2.** Controlled-potential electrolysis of *cis*-$[Ru(bpy)_2(NCCH_3)_2]^{2+}$ at −1.6 vs SSCE in CO_2-saturated 0.1 M TBAH/CH_3CN led to $[Ru(bpy)_2(CO_3)]$ after 2 electron equiv had been consumed. Under dinitrogen, 2 electron equiv were required for the reduction to reach completion. Reoxidation at −1.0 V led to the recovery of the starting bis(acetonitrilo) complex.

Insertion of CO_2. A solution of $[Ru(bpy)_2(CO)H](PF_6)$ (2.0×10^{-3} M) in 0.2 M TBAH/1,2-difluorobenzene with $[H_2O] \sim 10$ mM was reduced under a N_2 atmosphere at −1.4 V vs SSCE by 1 electron equiv. A red solution resulted with ν(CO) = 1901 cm^{-1} and λ_{max} = 494 nm (ϵ = 4920 M^{-1} cm^{-1}). Reoxidation at −1.0 V led to the complete recovery of *cis*-$[Ru(bpy)_2(CO)H]^+$. Upon slow addition of the red solution containing *cis*-$[Ru(bpy)_2(CO)H]^0$ to CO_2-saturated hexanes, the solution turned yellow. FTIR spectroscopy showed the presence of *cis*-$[Ru(bpy)_2(CO)H]^+$ (ν(CO) = 1938 cm^{-1}) and *cis*-$[Ru(bpy)_2(CO)(OC(O)H)]^+$ (ν(CO) = 1984 cm^{-1}) as products. The relative amounts of the products (typically ~66% *cis*-$[Ru(bpy)_2(CO)H]^+$ and ~33% *cis*-$[Ru(bpy)_2(CO)(OC(O)H)]^+$) were determined by integration of the areas under the ν(CO) bands.

Slow addition of a solution containing the reduced hydrido complex to acetonitrile saturated in CO_2 led to the complete recovery of $[Ru(bpy)_2(CO)H]^+$. In a related experiment, a 0.1 M KPF_6/CD_3CN solution containing *cis*-$[Ru(bpy)_2(CO)D]^+$ was reduced under N_2 by 1 electron equiv at −1.5 V to give *cis*-$[Ru(bpy)_2(CO)D]^0$. When CO_2 was bubbled through this red solution, its color changed to yellow. Partial conversion of *cis*-$[Ru(bpy)_2(CO)D]^+$ into *cis*-$[Ru(bpy)_2(CO)H]^+$ in the final product solution was confirmed by the appearance of a singlet at −11.5 ppm in the ^1H NMR spectrum. The chemical shift of the singlet coincided with that previously reported for the metal hydride resonance in *cis*-$[Ru(bpy)_2(CO)H]^+$.[4c] Reoxidation of *cis*-$[Ru(bpy)_2(CO)D]^0$ at −1.0 V, in the absence of CO_2, gave little or no evidence for the formation of *cis*-$[Ru(bpy)_2(CO)H]^+$ in control experiments.

Discussion

In previous work, it was shown that polypyridyl complexes of Ru and Os can act as electrocatalysts for the reduction of CO_2 to CO or formate.[1f,3,6] In the reduction of CO_2 catalyzed by *cis*-$[Os(bpy)_2(CO)H](PF_6)$ in CH_3CN with added water, both CO and formate were shown to appear as products by two separate mechanisms.[1f,g] Tanaka and co-workers have shown that when either *cis*-$[Ru(bpy)_2(CO)_2]^{2+}$ or *cis*-$[Ru(bpy)_2(CO)Cl]^+$ is reduced in the presence of CO_2, both CO and H_2 appeared as products in a 9:1 (v:v) H_2O:DMF mixture. When the acidity of the solution was decreased, formate anion also appeared as a product.[6c] We have demonstrated here that *cis*-$[Ru(bpy)_2(CO)H]^+$ is a catalyst for the reduction of CO_2 to CO and HCO_2^-. We have also acquired sufficient insight to propose a detailed mechanism for the reaction that leads to formate anion.

The key experimental observations which relate to mechanism are the following. (1) When CH_3CN solutions containing added H_2O and $[Ru(bpy)_2(CO)H]^+$ were electrolyzed in the presence of CO_2 at −1.3 or −1.6 V, formate and CO appeared as products. (2) At the end of the electrolysis period, *cis*-$[Ru(bpy)_2(CO)H]^+$, *cis*-$[Ru(bpy)_2(CO)(OC(O)H)]^+$, and *cis*-$[Ru(bpy)_2(CO)(NCCH_3)]^{2+}$ were all present in solution, as shown by FTIR spectroscopy. (3) Addition of a 1,2-difluorobenzene solution of the singly reduced hydrido complex, $[Ru(bpy)_2(CO)H]^0$, to a CO_2-saturated hexane solution gave *cis*-$[Ru(bpy)_2(CO)(OC(O)H)]^+$ and *cis*-$[Ru(bpy)_2(CO)H]^+$. Addition of $[Ru(bpy)_2(CO)D]^0$ to a CO_2-saturated CH_3CN solution led to $[Ru(bpy)_2(CO)H]^+$. (4) In the electrocatalyzed reduction of $^{13}CO_2$, there was no incorporation of ^{13}CO in the CO-containing complexes of Ru^{II}. (5) Two-electron reduction of either $[Ru(bpy)_2(CO)(OC(O)H)]^+$ or $[Ru(bpy)_2(CO)(NCCH_3)]^{2+}$ gave the hydrido complex by the reduction of water. (6) A loss of electrocatalytic activity with time coincided with the conversion of the CO-containing complexes into $[Ru(bpy)_2(CO_3)]$ or $[Ru(bpy)_2(NCCH_3)_2]^{2+}$.

Our observations point to the existence of four steps in the *cis*-$[Ru(bpy)_2(CO)H]^+$-catalyzed reduction of CO_2 to formate. In sequential order they are one-electron reduction, net insertion of CO_2 into the Ru–H bond, a second one-electron reduction, and re-formation of the hydrido complex by the reduction of water.

(1) Insertion. In the first step, one-electron bpy-based reduction of the complex occurs (eq 1). The addition of the electron enhances the electron density in the complex, which activates the

$$cis\text{-}[Ru(bpy)_2(CO)H]^+ + e^- \rightleftharpoons cis\text{-}[Ru(bpy)(bpy^-)(CO)H]^0 \quad (1)$$

$$cis\text{-}[Ru(bpy)(bpy^-)(CO)H]^0 + CO_2 \rightarrow cis\text{-}[Ru(bpy)_2(CO)(OC(O)H)]^0 \quad (2)$$

Ru–H bond toward the insertion of CO_2. The existence of the insertion chemistry (eq 2) was demonstrated by the appearance of the formato complex at the end of the electrolysis period and by the reaction between CO_2 and $[Ru(bpy)_2(CO)H]^0$ in hexanes/1,2-difluorobenzene which gave the formato complex as a product. On the cyclic voltammetric time scale, there was no evidence for a reaction between the reduced complex and added formate anion.

Addition of $[Ru(bpy)_2(CO)H]^0$ to CH_3CN saturated with CO_2 gave only *cis*-$[Ru(bpy)_2(CO)H]^+$. Confirmation that a net reaction had occurred under these conditions was obtained by the experiment with singly reduced *cis*-$[Ru(bpy)_2(CO)D]^+$, which gave *cis*-$[Ru(bpy)_2(CO)H]^+$ as the product. By inference, a complete catalytic cycle must have occurred under these conditions, with the slow step being the insertion of CO_2. Although other pathways may exist by which formate is produced, the insertion reaction does provide a mechanistic basis for explaining the appearance of formate anion in solution.

(2) Loss of Formate. The singly reduced formato complex, $[Ru(bpy)_2(CO)(OC(O)H)]^0$, is stable on the cyclic voltammetric time scale at a scan rate of 100 mV/s. A second reduction leads to the loss of formate anion and to the formation of the acetonitrilo complex (eqs 3, 4). At the potential for the insertion reaction, −1.35 V, the formato complex is reduced a second time and formate anion is lost.

$$cis\text{-}[Ru(bpy)_2(CO)(OC(O)H)]^0 + e^- \rightleftharpoons cis\text{-}[Ru(bpy)_2(CO)(OC(O)H)]^- \quad (3)$$

$$cis\text{-}[Ru(bpy)_2(CO)(OC(O)H)]^- + CH_3CN \rightarrow cis\text{-}[Ru(bpy)_2(CO)(NCCH_3)]^0 + HCO_2^- \quad (4)$$

Reduction of polypyridyl complexes of Ru^{II} or Os^{II} at bpy has been shown to labilize ligands. The rate of ligand loss was found to be greatly enhanced by two- as compared to one-electron reduction.[1a] From the scan rate dependent, cyclic voltammetric studies, in the absence of CO_2, loss of formate anion was complete in ≤0.1 s. Although the twice-reduced complex is written as the six-coordinate acetonitrilo complex in eq 4, we have no direct evidence that acetonitrile is bound and the complex could have a lower coordination number.

(3) Formation of the Hydride. The step that is required to complete the catalytic cycle is the reduction of water to re-form the hydride. The cyclic voltammograms in Figure 2 demonstrate that even at low levels of H_2O (1–5 mM), the hydrido complex is formed rapidly following the two-electron reduction of $[Ru(bpy)_2(CO)(NCCH_3)]^{2+}$ (eq 5). At a scan rate of 1000 V/s,

$$cis\text{-}[Ru(bpy)_2(CO)(NCCH_3)]^0 + H_2O \rightarrow cis\text{-}[Ru(bpy)_2(CO)H]^+ + OH^- + CH_3CN \quad (5)$$

the characteristic two-reduction pattern for $[Ru(bpy)_2(CO)$-

Scheme I

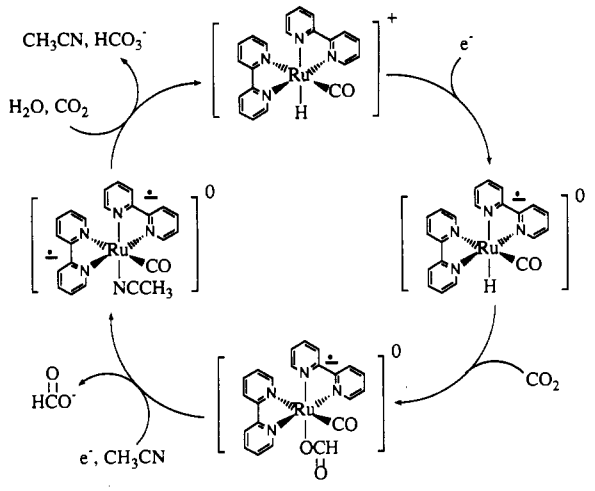

$(NCCH_3)]^{2+}$ was observed. At 100 mV/s, *cis*-$[Ru(bpy)_2(CO)H]^+$ appeared following reduction at the second wave. From scan rate studies, the hydrido complex appears on a time scale of ~2 ms at $[H_2O] \sim 1$ mM.

From the experiments in 1,2-difluorobenzene, where two-electron reduction of *cis*-$[Ru(bpy)_2(CO)(OC(O)H)]^+$ gave *cis*-$[Ru(bpy)_2(CO)H]^+$, it is not possible to invoke eq 5 as the sole pathway for formation of the hydride. Direct reduction of H_2O by the twice-reduced formato complex (eq 6), or even a lower

$$cis\text{-}[Ru(bpy)_2(CO)(OC(O)H)]^- + H_2O \rightarrow cis\text{-}[Ru(bpy)_2(CO)H]^+ + OH^- + HCO_2^- \quad (6)$$

coordinate twice-reduced intermediate may also contribute. There is no direct way to distinguish among eq 6, a mechanism involving eq 4 followed by eq 5, and a common, lower coordinate intermediate. Even under our most dehydrated conditions, ~1 mM H_2O, formation of the hydride was more rapid than loss of formate by a factor of ~50.

The series of reactions (1)–(5) constitute a catalytic cycle in which CO_2 is reduced to formate anion. The cycle is illustrated in Scheme I. As noted above, we have no direct evidence that the twice-reduced complex contains bound acetonitrile. When combined with the acid–base reaction between OH^- and CO_2 to give HCO_3^- (eq 7), these reactions add up to give the half-cell

$$OH^- + CO_2 \rightarrow HCO_3^- \quad (7)$$

$$2CO_2 + H_2O + 2e^- \xrightarrow{[Ru(bpy)_2(CO)H]^+} HCO_2^- + HCO_3^- \quad (8)$$

reaction in eq 8. It is the half-cell reaction in eq 8 that is catalyzed by the complex.

Other Pathways for the Reduction of CO_2. From the appearance of CO as a coproduct, it can be inferred that an additional pathway for the reduction of CO_2 must exist. In an earlier series of experiments it was demonstrated that electrochemical reduction of *cis*-$[Os(bpy)_2(CO)H]^+$ or related *cis*-alkyl complexes of Os^{II} in the presence of CO_2, led to both CO and formate.[1f,g] These complexes reduce CO_2 by a different pathway. A two-electron reduction was required, and neither the carbonyl nor the hydrido ligand initially in *cis*-$[Os(bpy)_2(CO)H]^+$ appear in the CO or formato products. It was concluded that the reactions occur by associative attack of CO_2 at the metal in the reduced complexes, followed by the formation of CO or formate by different intermediates.[1f,g]

The controlled-potential electrolysis experiments based on *cis*-$[Ru(bpy)_2(CO)(CH_2Ph)]^+$ demonstrated that this complex shares with the complexes of Os^{II} the ability to act as an electrocatalyst toward the reduction of CO_2 to give CO and formate. From the absence of *cis*-$[Ru(bpy)_2(CO)H]^+$ and *cis*-$[Ru(bpy)_2(CO)(CO_2CH_2Ph)]^+$ as products at the end of the electrolysis period, it can be concluded that insertion of CO_2 into the Ru–C bond does not occur. On the basis of these observations, the associative two-electron reduction pathway appears to be operative for the benzyl complex of Ru^{II} as well.

Either *cis*-$[Ru(bpy)_2(CO)(OC(O)H)]^+$, *cis*-$[Ru(bpy)_2(CO)(NCCH_3)]^+$, or both could be the catalyst for the CO-producing pathway. Both are reduced by two electrons in the potential range used for the electrolyses. Although the associative attack pathway is probably the origin of CO as a product, it may also contribute to the production of formate anion.

The reduction of CO_2 by *cis*-$[Ru(bpy)_2(CO)Cl]^+$ or *cis*-$[Ru(bpy)_2(CO)_2]^{2+}$ has been proposed to occur by addition of OH^- to bound CO to give metallo carboxylato intermediates, followed by reduction.[6c] This mechanism can be ruled out for *cis*-$[Ru(bpy)_2(CO)H]^+$, as can others that involve the bound CO group as the origin of formate. This conclusion is based on the absence of ^{13}C-labeled CO in the catalyst in the electrolysis experiment involving $^{13}CO_2$. The absence of a ^{13}CO label is consistent with either CO_2 insertion into the Ru–H bond or associative attack. The innocence of the CO ligand is somewhat surprising given the failure of *cis*-$[Ru(bpy)_2(NCCH_3)_2]^{2+}$ or of $[Ru(bpy)_2(CO_3)]$, which are non-CO containing, to catalyze the reduction of CO_2. The role of the CO ligand must lie elsewhere. It is probably in the electronic stabilization at the metal provided by back-bonding and the role that it plays in the formation and stabilization of the hydride.

There is a notable contrast in reactivity toward CO_2 among the three hydrides, *fac*-$[Re(bpy)(CO)_3H]$ and *cis*-$[M(bpy)_2(CO)H]^+$ (M = Ru, Os). For the Re complex, insertion occurs at a reasonable rate in solution at room temperature.[3c] For the Ru complex, insertion requires activation by initial one-electron reduction at bpy. For the Os complex, activation, at least on the time scale of the cyclic voltammetric experiments, does not occur until the complex is twice-reduced. Reduction of CO_2 by Os then occurs by the associative attack mechanism, and there is no sign of insertion. The contrast in behavior may be a reflection of both the relative basicities and strengths of the metal–hydride bonds.[12] For the twice-reduced Os complex, the activation barrier to insertion must be too high to compete with the associative pathway.

As noted in the experimental section, the singly reduced hydrido complex is not a facile catalyst for the reduction of water to H_2 in CH_3CN solutions, at least at low concentrations of H_2O. The reduced complex is stable in 1 mM H_2O/CH_3CN over a period of several hours. The stability may be the result of the low concentration of water since $[Ru(bpy)_2(CO)H]^+$ has been reported to be a water reduction catalyst in acidic aqueous solution.[4a]

Deactivation of the Catalyst. The electrocatalytic activity of *cis*-$[Ru(bpy)_2(CO)H]^+$ decreased slowly over an extended period. The loss in catalytic activity was paralleled by the disappearance of the carbonyl-containing complexes and the growth of $[Ru(bpy)_2(CO_3)]$. The carbonato complex appeared following the two-electron reduction of *cis*-$[Ru(bpy)_2(NCCH_3)_2]^{2+}$ in the presence of CO_2 and OH^-. Presumably, the appearance of *cis*-$[Ru(bpy)_2(NCCH_3)_2]^{2+}$ has its origin in the reductively induced loss of CO from *cis*-$[Ru(bpy)_2(CO)(NCCH_3)]^{2+}$. As noted above, neither the bis(acetonitrilo) complex nor the carbonato complex are catalysts for the electrochemical reduction of CO_2.

Conclusions

The key steps in the electrocatalyzed reduction of CO_2 to formate are reductively induced insertion into the Ru–H bond and re-formation of the metal hydride by the reduction of water. Although both reactions are known, to our knowledge, this is the first demonstration of their intervention in a catalytic cycle.

Both the insertion and the two-electron, associative attack mechanisms rely on interactions between the reduced complexes and CO_2 acting as an electrophile. Both are activated by initial reductions at π^*(bpy), and these ligand-based reductions have a profound effect on reactivity. They increase the electron density both at the metal and at the metal–hydride bond. The enhanced electron density at the metal in *cis*-$[Os(bpy)_2(CO)H]^-$ opens a reactivity channel based on associative attack by CO_2 as an electrophile. The electron-enriched Ru–H bond in *cis*-[Ru-

$(bpy)_2(CO)H]^0$ has an enhanced susceptibility toward insertion by CO_2. These electronic influences lie at the heart of the reactivity of these complexes. When combined with the ability to re-form the metal–hydride bond, they provide the mechanistic basis for the electrocatalyzed reduction of CO_2.

Acknowledgment. Funding by the Office of Naval Research under Contract No. N00014-87-K-0430 and the Gas Research Institute under Contract No. 5087-260-1455 is gratefully acknowledged. We also thank Dr. Martha Reynolds for help in acquiring the NMR data.

Contribution from the Inorganic Chemistry Laboratory, University of Oxford, South Parks Road, Oxford OX1 3QR, United Kingdom

Closed-Shell Electronic Requirements for Condensed Clusters of the Group 11 Elements

Zhenyang Lin, Renê P. F. Kanters, and D. Michael P. Mingos*

Received February 5, 1990

The bondings in two limiting types of spherical gold clusters are considered in this paper. Close-packed spherical gold clusters form molecular orbitals that can be analyzed by using the jellium model. Closed shells correspond to the filling of the following wave functions: 1s, 1p, 1d, 2s, 1f, 2p, 1g, etc., which have been defined with pseudospherical symmetry labels. In the more open structures based on vertex-linked icosahedra, the molecular orbitals correspond to the summation of the S^σ and P^σ molecular orbitals associated with each icosahedron. Therefore, the closed-shell requirements correspond to $8n_p$ electrons, where n_p = the number of icosahedra. These closed shells result because the orbital interactions between icosahedra are much smaller than those within a single icosahedron. The more open linked icosahedral packing mode results in a greater utilization of electrons per gold atom than the more densely packed structures. The jellium analysis appears to be appropriate for describing the closed-shell requirements for gold clusters that have been studied in molecular beams but fails when applied to vertex-shared icosahedra. The closed-shell configurations of the latter are, however, satisfactorily analyzed by using the additive model based on the bonding requirements of the individual icosahedra.

Introduction

Molecular clusters, which can be either bare in molecular beam experiments or ligated in solid-state and solution experiments, have attracted considerable interest recently.[1] A jellium model has been developed to account for the electronic structures of bare clusters produced in molecular beams.[2] This model has successfully predicted several of the magic numbers in mass spectral data for alkali-metal clusters by associating their nuclearities with closed-shell electronic configurations for a particle in a sphere model. A crystal field perturbation analysis, which has been described as a structural jellium model, has led to the conclusion that alkali-metal clusters with closed-shell electronic configurations based on the jellium model adopt, when possible, high-symmetry (T_d, O_h, or I_h point group) structures based on close-packed or nearly close-packed spherical geometries.[3] It has also been demonstrated that the jellium model is closely related to the tensor surface harmonic theory[4] developed for transition-metal and main-group clusters.[5]

Ligated clusters provide some examples of these close-packed situations, but also less symmetrical clusters based on vertex, edge, and face sharings. In their formation, kinetic effects associated with the inertness of the metal–ligand bonds lead to the adoption of these more open metal structures in preference to close-packed arrangements. The closed-shell requirements of these clusters are well established through the polyhedral skeletal electron pair theory (PSEPT),[6] which provides relationships between the skeletal structure and the total number of valence electrons in the cluster. The tensor surface harmonic theory[4] provides a theoretical justification for these structural relationships. Other approaches to cluster bonding have been proposed by King[7] and Teo.[8] These simple rules, however, do not work well for metal clusters derived from s^1 configuration metals (e.g. alkali and group 11 metals), e.g. for Au and Ag ligated clusters.

The detailed understanding of the electronic structures in gold ligated clusters has been limited to those clusters of the type $[(AuPR_3)_n]^{x+}$ (n = 4–7)[9] and the centered clusters $[Au(AuPR_3)_n]^{x+}$ (n = 8–12).[10] In the former, the Au atoms are located approximately on a single sphere, whereas the latter have one Au atom in the center. It has been demonstrated that the bonding in these gold cluster compounds can be described in terms of the interactions between radially hybridized (s–z) orbitals of the $AuPR_3$ fragments. The following closed-shell requirements have been derived from extended Hückel molecular orbital calculations and the tensor surface harmonic theory (TSH):[4]

	tot. no. of valence electrons	no. of metal s electrons	
$[Au(AuPR_3)_n]^{x+}$	$12n + 18$	8	if the n surface gold atoms lie approximately on a sphere
	$12n + 16$	6	if the surface gold atoms adopt a toroidal or elliptical arrangement
$[(AuPR_3)_n]^{x+}$	$12n + 2$	2	spherical geometry
	$12n + 4$	4	prolate geometry
	$12n + 6$	6	oblate geometry
	$12n + 8$	8	spherical geometry

(1) Jena, P., Rao, B. K., Khanna, S. N., Eds. *Physics and Chemistry of Small Clusters*; NATO ASI Series B, Vol. 158; NATO Advanced Study Institute: New York, 1987.
(2) Knight, W. D.; Clemenger, K.; de heer, W. A.; Saunder, W. A.; Chou, M. Y.; Cohen, M. L. *Phys. Rev. Lett.* **1984**, *52*, 2141.
(3) Lin, Z.; Slee, T.; Mingos, D. M. P. *Chem. Phys.* **1990**, *142*, 321.
(4) (a) Stone, A. J. *Mol. Phys.* **1980**, *41*, 1339. (b) Stone, A. J. *Inorg. Chem.* **1981**, *20*, 563. (c) Stone, A. J. *Polyhedron* **1980**, *3*, 1229.
(5) Mingos, D. M. P.; Johnston, R. *Struct. Bonding* **1987**, *68*, 29.
(6) Mingos, D. M. P. *Chem. Soc. Rev.* **1986**, *15*, 31.
(7) King, R. B. In *Chemical Applications of Topological and Graph Theory*; King, R. B., Ed.; Elsevier: Amsterdam, 1983; pp 99–123.
(8) (a) Teo, B. K. *Inorg. Chem.* **1984**, *23*, 1251. (b) Teo, B. K. *Inorg. Chem.* **1985**, *24*, 1627. (c) Teo, B. K. *Inorg. Chem.* **1985**, *24*, 4209. (d) Teo, B. K.; Sloane, N. A. J. *Inorg. Chem.* **1985**, *24*, 4545. (e) Sloane, N. A. J.; Teo, B. K. *J. Chem. Phys.* **1985**, *83*, 6520. (f) Teo, B. K.; Sloane, N. A. J. *Inorg. Chem.* **1986**, *25*, 2315.
(9) Evans, D. G.; Mingos, D. M. P. *J. Organomet. Chem.* **1982**, *232*, 171.
(10) Mingos, D. M. P.; Hall, K. P.; Gilmour, D. I. *J. Organomet. Chem.* **1984**, *268*, 275.

0020-1669/91/1330-0091$02.50/0